NÖHÜ Müh. Bilim. Derg. / NOHU J. Eng. Sci., 2025; 14(3), 1155-1170

Niğde Ömer Halisdemir Üniversitesi Mühendislik Bilimleri Dergisi
Niğde Ömer Halisdemir University Journal of Engineering Sciences

Derleme makalesi / Review article

www.dergipark.org.tr/tr/pub/ngumuh / www.dergipark.org.tr/en/pub/ngumuh

A review on strategies for minimizing cogging torque in flux-switching permanent magnet machines

Akı anahtarlamalı sabit mıknatıslı makinelerde vuruntu momentini en aza indirme stratejileri üzerine bir inceleme

Başak Tepretmez[1,*], Emrah Çetin[2]

[1,2] *Tarsus University, Electrical and Electronic Engineering Department, 33400, Mersin, Türkiye*

Abstract

Due to high volume of the studies in the field, flux switching permanent magnet (FSPM) machines are explored in this article. Particularly, this paper is examined the studies carried out to reduce cogging torque (CT) in FSPMs. The reduction of CT improves the smoothness and efficiency of electric machines, improving the effectiveness of control systems. In addition, the reduction in vibration and noise levels increases accuracy and reliability, particularly in sensitive applications. The research begins with a systematic examination of CT in FSPM machines. Through this analysis, certain parameters contributing to the mitigation of CT were determined, and relevant advancements from prior literature were thoroughly examined. Mostly, the structural changes were implemented by enhancing the rotor and stator to mitigate the CT. The rotor and stator efforts are discussed and classified in detail in this paper. These investigations substantiate the degradation in CT and the results make a significant contribution to the existing literature within the scope.

Keywords: CT, Flux switching machine, Optimization, Permanent magnet, Rotor/Stator

Öz

Bu alandaki çalışmaların yoğunluğu nedeniyle, bu makalede akı anahtarlamalı sabit mıknatıslı (AASM) makineler incelenmiştir. Bu makalede özellikle AASM'lerde vuruntu momentini (VM) azaltmak için yapılan çalışmalar incelenmiştir. VM'nin azaltılması, elektrik makinelerinin düzgünlüğünü ve verimliliğini artırarak kontrol sistemlerinin etkinliğini geliştirir. Buna ek olarak, titreşim ve gürültü seviyelerindeki azalma, özellikle hassas uygulamalarda doğruluğu ve güvenilirliği artırır. Araştırmalar, AASM makinelerindeki vuruntu momentini sistematik bir şekilde incelemesiyle başlamaktadır. Bu analizin sonucunda VM'yi azaltmayı amaçlayan parametreler belirlenmiş ve ilgili iyileştirme çalışmaları gözden geçirilmiştir. Çoğunlukla, yapısal değişiklikler vuruntu momentini azaltmak için rotor ve statoru geliştirerek uygulanmıştır. Rotor ve stator çalışmaları makalede ayrıntılı olarak tartışılmış ve sınıflandırılmıştır. Bu incelemeler VM'yi azaltmayı kanıtlamakta ve sonuçlar bu kapsamdaki mevcut literatürde önemli bir katkı sağlamaktadır.

Anahtar Kelimeler: Vuruntu momenti, Akı anahtarlamalı makine, Optimizasyon, Sabit mıknatıs, Rotor/Stator

1 Introduction

Electric machines that enhance energy conversion through magnetic influences use the exchange of magnetic fields between permanent magnets (PMs) on the stator and the cogging, moving structure of the rotor. Flux-switching permanent magnet (FSPM) electrical machines operate through magnetic interactions between the windings and permanent magnets (PMs) on the stator, which generate a constant magnetic field, and the toothed, movable structure of the rotor [1]. A switching distinction between flux-switching permanent magnet machines and PM-assisted synchronous reluctance machines lies in the placement of the magnets; FSPMs incorporate the magnets within the stator and utilize a dual excitation system Figure 1 [2]. In such machines, the stator generates magnetic flux, and the rotor's capability to guide the magnetic circuit optimizes energy conversion through flux switching.

The design of FSPM machines (FSPMMs) is of paramount importance in the field of electrical engineering. Analyses conducted through finite element analysis (FEA) elucidate this significance further. FSPMMs are appealing for the electric machine designers due to the electromagnetic and electromechanical characteristics of it. Such as high-power density [3,4], high torque capability [5], primary topology on rotor [6], sinusoidal back electromotive force [7,8] etc. However, one of the consequences of this appealing profile, high CT occurs in FSPMs [9] and that needs to be handled. Thus, most of the researchers focus on the investigations into the mitigation of CT.

The most important challenge in FSPMM is CT, which effect out of magnetic influences among the rotor and stator at certain positions. Due to their dual salient structure, FSPMMs generate high levels of CT, leading to resistance in rotor rotation, increased vibration, and noise. These effects are particularly problematic in particular applications. To

* Sorumlu yazar / Corresponding author, e-posta / e-mail: 240929005@tarsus.edu.tr (B. Tepretmez)
Geliş / Received: 18.12.2024 Kabul / Accepted: 06.05.2025 Yayımlanma / Published: 15.07.2025
doi: 10.28948/ngumuh.1603645

improve performance and efficiency, reducing CT through optimized design and manufacturing processes is essential. [10]

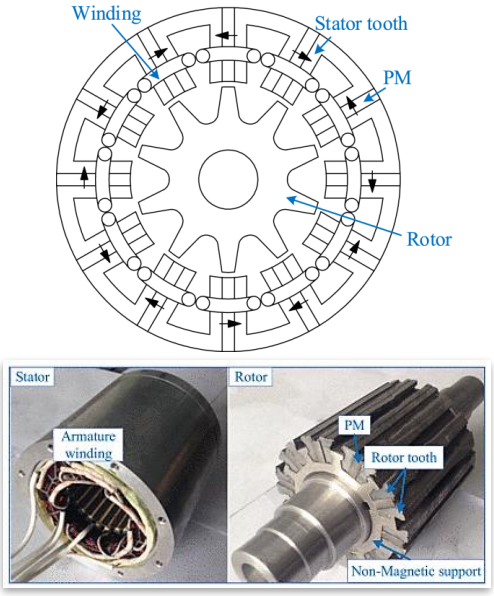

Figure 1. Conventional FSPM machine topology and the prototype [2]

The reduction of CT emerges as a critical objective for enhancing the performance, efficiency, and durability of electric machines. Relevant studies not only have the potential to improve machine performance by providing higher energy efficiency and longer lifespan but also contribute to the smoother management of machine dynamics. The resulting reduction in CT is considered a fundamental element for innovation and advancement in the field of electrical machines. Due to having the permanent magnets, the CT mitigation is very crucial for FSPMs.

Researchers have investigated numerous methods for reducing CT. Some of these methods focus on the stator side, such as magnet placement and design, as well as winding patterns [11,12]. Others are concentrated on the rotor side, including variations in rotor pole arc angles, widths, and shaping [13–17]. Many studies emphasize the combined effects of both the rotor and stator through various structural combinations [18–20]. In addition, some research has explored motor control strategies to mitigate CT. Various approaches based on harmonic current injection (HCI) and iterative learning control (ILC) have recently been proposed to compensate for and modulate the air gap flux density [21,22]. Moreover, topological changes such as increasing the number of phases have also been shown to effectively reduce torque ripple, which is closely associated with CT.

The studies on the CT mitigation reveal that magnetic interactions, structural design parameters, air gap configurations, and winding arrangements significantly effect the magnetic field and consequently the CT [23,24]. Each of these factors plays a pivotal role in the determination of CT, positioning them as critical elements that influence the generally execution of the machine.

In this study, the latest advances in approaches developed for the decrease of CT in FSPMMs are comprehensively examined. The paper is organized to provide a clear and systematic exploration of the topic. Section II begins with a detailed explanation of the analytical methods used to understand the mechanisms behind CT generation in FSPM machines, offering a foundation for the techniques discussed later. Following this, Section III presents an extensive review of state-of-the-art methods and strategies proposed for effectively reducing CT, highlighting their principles, applications, and potential benefits. Lastly, the conclusion section provides a summary of the findings and a critical discussion of the challenges, practical implications, and future directions for CT mitigation in FSPMMs.

2 CT Expression

2.1 Methodology

In this review, a comprehensive literature survey was conducted to identify and analyze various strategies developed to minimize CT in FSPM machines. The review focused on peer-reviewed journal articles, conference proceedings, and relevant academic sources published between 2005 and 2025.

Sources were selected based on their relevance to CT reduction methods in FSPM machines, including both analytical and experimental studies. Databases such as IEEE Xplore, ScienceDirect, and Google Scholar were primarily used to gather the literature. Keywords including "CT reduction", "flux-switching permanent magnet", "magnetic design optimization", and "machine topology modification" guided the search process.

The selected papers were categorized based on the type of technique they proposed—such as rotor/stator geometry modifications, magnet shifting, pole arc optimization, or auxiliary slot introduction. Comparative evaluations were also considered to highlight the strengths and limitations of each approach.

This methodology ensured a structured and focused review of the existing body of knowledge, enabling a well-informed discussion on the effectiveness and applicability of various CT mitigation strategies in FSPM machines.

The principles of working FSPM machines are interesting in view of magnetic flux orientation and torque generation. The CT generated in the FSPMM can be represented as the rate of the change of the magnetic co-energy with repaired the machine, as expressed in Equation (1), where α denotes the rotor displacement angle and has an active function in maintaining the torque creation of the machine.

$$T_{cog} = -\frac{\partial W}{\partial \alpha} \tag{1}$$

Here α symbol is the specify rotor position. As a result of the transmittance of iron core is considerably stronger than that of the air-gap and PMs, the magnetic co-energy W, can be exchanged with W_{gap}, deposited in the air-gap, thus the energy change in the iron core ignoring. [25]

$$W \approx W_{gap} = \frac{1}{2\mu_0}\int_V B^2(\theta)dV = \frac{1}{2\mu_0}\int_V B_r^2(\theta)G^2(\theta,\alpha)dV \quad (2)$$

Depending on the angle θ along the perimeter of the air gap depicted in Equation (2), the flux density delivery B(θ) along the air gap, the flux density delivery developed by the PMs at the stator is denoted by $B_r(\theta)$, and the impact of the prominent rotor on the flux density stator is denoted by G (θ, α). The Fourier expansion and analytical prediction of $B_r^2(\theta)$ for the real case are given in Equation (3) respectively.

$$B_r^2(\theta) = B_{r0} + \sum_{m=1}^{\infty} B_{rm} \cos m P_s \theta \quad (3)$$

The Fourier expansion of $G^2(\theta, \alpha)$ is given by:

$$G^2(\theta,\alpha) = G_0 + \sum_{n=1}^{\infty} G_n \cos n P_r(\theta + \alpha) \quad (4)$$

$$T_{cog}(\alpha) = \frac{\pi P_r L_{Fe}}{4\mu_0}(R_2^2 - R_1^2)\sum_{n=1}^{\infty} nG_n B_{r\frac{k_{mn}}{P_s}} \sin k_{mn}\alpha \quad (5)$$

L_{fe} here denotes the axial arrange distance, R_1 and R_2 indicate the outer radius of rotor and the inner radius of the stator in the same order. Where,

$$k_{mn} = nP_r \ \ or \ \ k_{mn} = nP_r = 2mP_s \quad (6)$$

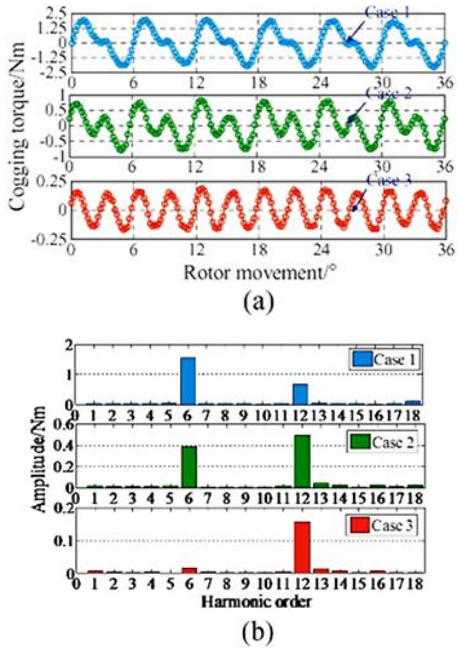

Figure 2. (a) CT waveforms, (b) harmonic order for three different cases [25]

As shown in Equation (5) the CT cycle generated within an individual rotor phase should include the smallest possible number of cycles. For instance, despite using the similar quantity of stator and rotor poles, CT has been calculated for three cases in the study [25]. As demonstrated in Figure 2, Case 1 shows the original configuration, whereas in Cases 2 and 3, PMs with reduced spacing and lower magnetic energy are employed. The waveform and harmonic structure of the CT for these three cases have been analyzed [25].

According to the Equation (5), Tcog can be reduced through the model of the stator or the rotor design. This mitigation can be achieved by using various methods, but most of them focus on the air gap permeance manipulation.

3 CT Reduction techniques

In this section, the methods used to reduce CT in FSPM machines will be examined, focusing on both rotor and stator components. It includes common improvements in rotor and stator designs to facilitate CT reduction through various optimization techniques and structural changes.

3.1 Rotor side adjustment

The rotor is the moving part of FSPM machines. There are various methods to reduce CT on the rotor side of FSPMMs. These methods include optimizing the rotor geometry [26], designing the rotor with axial skew [27], chamfering the rotor tooth tips [28], and segmenting the rotor slots [29]. These strategies support the effective minimization of CT through refinements in rotor configuration. The optimization techniques applied to the rotor side are summarized along with their corresponding references in Table 1 for clarity and comparison.

Table 1. Rotor side adjustments

ROTOR ADJUSTMENT	REFERENCE
3-D end effect and rotor eccentric, rotor optimization	[3,15,30,31]
Shifting rotor teeth, and stepped skewing rotor blocks	[16]
Rotor pole shaping, chamfering and flange rotor pole shape without skewing teeth	[7,27,32]
Teeth notching	[25,33]
Rotor pole width Rotor pole shape Rotor pole skew Rotor pole displacement Rotor dummy slot	[29,34]
Different arc angled rotor poles	[35,36]
Skewing, step-skewing, notching, pairing, right-angle chamfering and cos-chamfering rotors	[27,28,37]
Rotor position	[18,38]
External rotor	[39,40]
Different rotor tooth	[41]
Outer Rotor Structure	[42]

The author in study [35] the design of the Unequal Rotor Slot Arc (URSA), which investigates the effects of asymmetric rotor poles with distinct angles for a three phase FSPM machine. During the configuration process, an FSPM machine topology consisting of 12 stator poles and 10 rotor poles was selected. The results show that the unequal rotor slot arcs exhibit superior performance compared to the symmetrical design. The asymmetric schemes for the rotor slots were, simulated using parametric analysis to reduce the CT. Figure 3 illustrates the angle parameter in the parametric optimization process. To achieve optimization, two angles, θ_a and θ_b are defined, which can adjust the rotor pole as depicted in Figure 4. When equal rotor slot angles are accepted as zero, the unequal rotor slot angles are constrained between plus and minus two degrees to facilitate the optimization process. Additionally, an inequality is established for the two consecutive rotor poles, allowing the angles θ_{rs1} and θ_{rs2} to vary by ± 2 degrees. The proposed design shows a significant reduction in CT and shows a significant improvement.

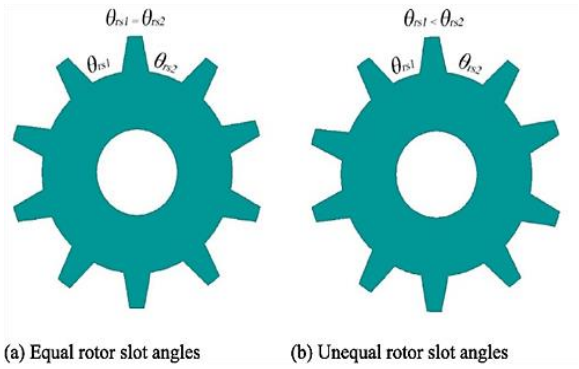

Figure 3. The configuration of the URSA method for FSPMs [36]

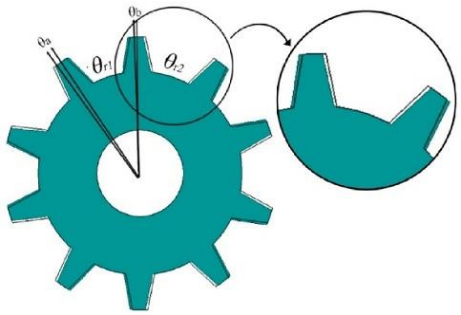

Figure 4. Unequal rotor slot angles method and optimization process angle parameters [36]

Five distinct angles have been selected to present the results in a comparative manner. The chosen angle parameters are detailed in Table 2.

$$\theta_{r1} = \theta_{rs1} \pm \theta_a$$
$$\theta_{r2} = \theta_{rs2} \pm \theta_b \quad (7)$$

Table 2. Chosen angle parameters after the FEA optimization process [36]

	θ_a	θ_b
Design 1 (D1)	1.2	-2
Design 2 (D2)	1.4	-1.8
Design 3 (D3)	-2	1.1
Design 4 (D4)	0.8	-2
Design 0 (D0)	0	0

The proposed design shows a significant reduction in CT and shows a significant improvement in [36]. Figure 5 highlights the impactivity of the URSA method in minimization CT, establishing it as a pioneering solution. According to the optimization and simulation results, D1 exhibits the lowest CT at 4.1% and also demonstrates a reasonable average torque loss. These findings support the assertion that the URSA method has significant potential for mitigating CT. Ultimately, the employment of unequal rotor slot arcs for FSPMMs allows satisfactory results to be achieved.

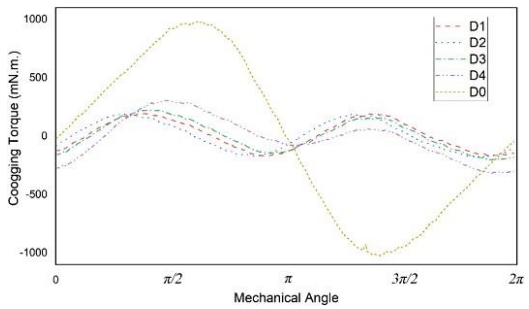

Figure 5. CT results [36]

Xiu et. al. proposed a new chamfered and flanged rotor pole geometry to reduce the CT without the use of sloping teeth [32]. The basic recommended dimensions of the rotor pole geometry have been optimized Figure 6. It shows the contribution of this pole shape to CT reduction by providing a more stepped change in the air gap opposition in the magnetic flux direction during rotor spinning. This impact of the method is confirmed by FEA and modeling based on practical examples. The influences of the offered pole configuration on the reverse electromotive force (EMF) and average electromagnetic torque are moreover studied. On a 6/4 pole FSPM machine, it is critical to reduce the CT to a certain low level to ensure the smooth machine operation. In this context, a chamfered and flanged rotor pole geometry without chamfered teeth is proposed. The proposed pole geometry is optimized by systematic techniques and FEA founded simulations, and the effectiveness of the approach is verified with empirical data.

In addition, the effects of this novel pole shape on the back EMF and the average electromagnetic torque are evaluated in detail. For a constant air gap distance, an unexpected alteration in air gap transmittance as the rotor pole side joins or exits the stator pole. But, in case of a larger air gap is added when the poles begin to overlap, this sudden change can be reduced. As the air gap length gradually

decreases, the air gap permeance changes more smoothly, lowering CT. For this reason, a chamfered rotor pole surface is recommended. This creates a gradual rise in the air gap from the center to the edge, allowing a smoother variation in air gap permeance. Accordingly, the circulation of $G^2(\alpha, \theta)$ down the perimeter of the edge rounding rotor pole area is displayed in Figure 6b [32].

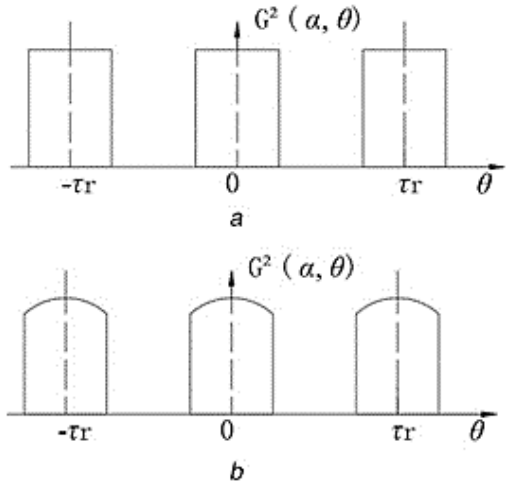

Figure 6. G(α,θ) distribution (a) Fixed air gap distance, (b) Edge rounding rotor pole surface [32]

In this study, a chamfered and flanged rotor pole design is presented in Figure 7. This design provides a further incremental change of air gap displacement in the flux linkage during rotor rotation, which results in lower CT.

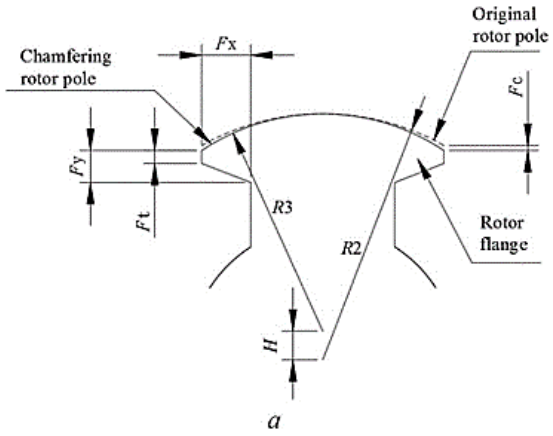

Figure 7. Suggested chamfering and flange rotor pole form [32]

To provide more analytical conclusions, the optimum dimensions of the flange thickness (F_x) and flange height (F_y) are considered using the Finite Element (FE) technique, which effectively allows to take into account for magnetic fullness and flux escape effects. As the FE study, the flange width (F_x) and flange height (F_y) are made equal, while the flange edge thickness F_t is kept at constant value. The simulation of FE analysis for the CT of the recommended rotor pole configuration with various chamfer magnitude and flange width dimensions are given in Figure 8.

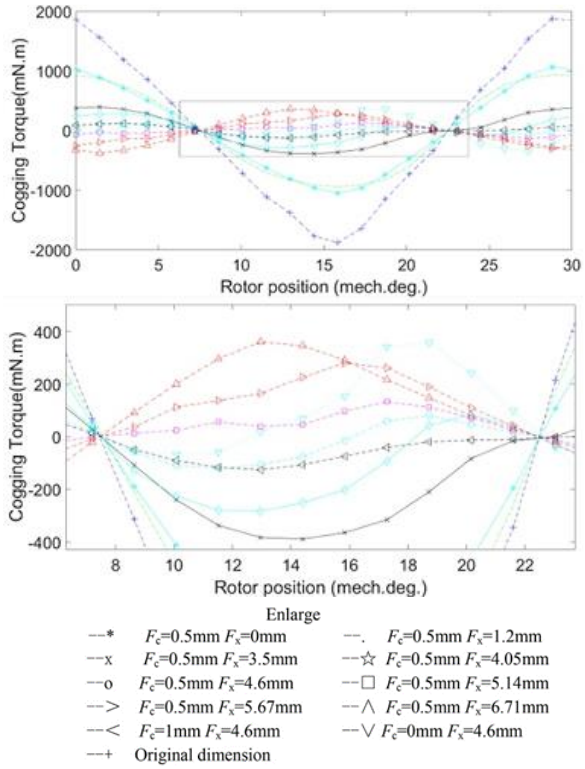

Figure 8. CT from the new rotor pole configuration by various scales of chamfer magnitude and flange width sizes [32]

Zhang et. al. [37] examine six rotor-side cogging suppression methods to improve the efficiency of FSPM machines. These methods include skewing, step-skewing, notching, pairing, right-angle chamfering and cos-chamfering rotors, as depicted in Figure 9. The skewed rotor technique [Figure 9(a)] reduces torque ripple by tilting the rotor core at a specific angle. The step-skewed [Figure 9(b)] rotor is a more effective version of this method. The notched [Figure 9(c)] rotor reduces harmonics causing torque ripple by adding notches to the rotor teeth. The paired [Figure 9(d)] rotor suppresses torque ripple by alternating rotor teeth of different widths, modulating the magnetic field. Right-angle [Figure 9(e)] and cos-chamfered [Figure 9(f)] rotor methods apply chamfers of different shapes to the rotor teeth tips to reduce torque ripple. While all these techniques minimize torque ripple, they also impact other performance factors like back EMF and torque. Therefore, the most suitable method should be chosen based on application requirements. Their robustness against manufacturing errors has also been considered.

Using FEA, the study predicts the effect of each technique on the CT waveforms of the FSPMM to assess the effectiveness of CT repression. Moreover, the outcomes of the methods applied to reduce the CT are demonstrated in Figure 10.

Furthermore, an overall theoretical analysis is conducted out to illuminate the common characteristics of cogging minimization techniques in FSPM machines. The observations contribute to a more integrated rotor structure methodology for researchers and designers in the field. In

addition, prototype experiments are carried out on a 12s/10p FSPMM utilizing four of the above rotor strategies. The observation of these experiments supplies important reference points for cogging suppression strategies applicable to FSPM machines.

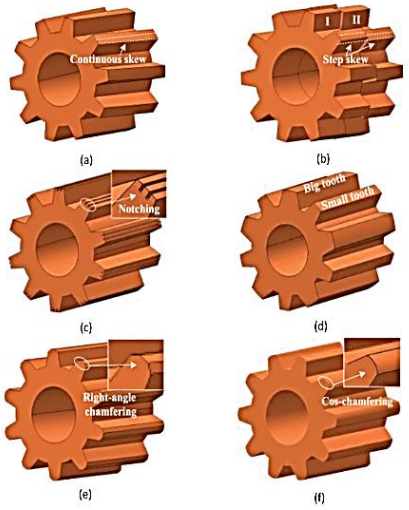

Figure 9. CT of the 12s/10p FSPMM with the rotors (a) continuous skew, (b) step-skew, (c) notching, (d) big/small tooth content, (e) right-angle chamfering, (f) chamfering [37]

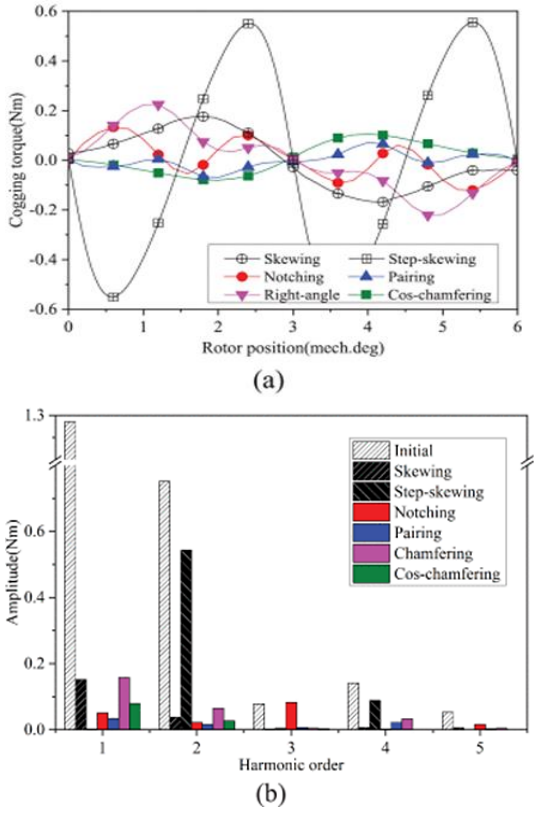

Figure 10. CT of the 12s/10p FSPMM with the rotors (a) CT waveforms (b) Harmonic analysis of the torque content [37]

3.2 Stator side adjustment

In this study, the latest advances in approaches developed for the decrease of CT in FSPMMs are comprehensively examined. The paper is organized to provide a clear and systematic exploration of the topic. Section II begins with a detailed explanation of the analytical methods used to understand the mechanisms behind CT generation in FSPM machines, offering a foundation for the techniques discussed later. Following this, Section III presents an extensive review of state-of-the-art methods and strategies proposed for effectively reducing CT, highlighting their principles, applications, and potential benefits. For ease of comparison and reference, these techniques along with their corresponding literature sources are systematically compiled in Table 3. Lastly, the conclusion section provides a summary of the findings and a critical discussion of the challenges, practical implications, and future directions for CT mitigation in FSPMMs.

Table 3. Stator side adjustments

STATOR ADJUSTMENT	REFERENCE
Different permanent magnet materials	[4]
Stator flux bridges Stator structure effects of short permanent magnets	[43,44]
Winding configuration	[23,45]
A new pole shaping	[46]
Distinct stator/rotor pole arrangements Winding arrangements and stator layering section forms	[47,48]
Dummy slot	[49,50]
Hybrid excited multi-tooth	[51]

Gan et. al. investigates the reduction of CT in three phase 12s/10p FSPMMs by examining the impact of compact permanent magnets and stator flux bridges (FB) in [43]. Four diverse FSPM configurations (outer/inner, inner/inner, inner/outer and outer/outer) Figure 11. were developed by adjusting FB placement and PM length. Through finite-element analysis, CT, output torque, and PM usage were compared across configurations. Experimental validation confirmed that the outer-inner structure effectively reduces CT and decreases PM material usage.

The segmented and modular design of the stator core complicates assembly. To make the stator more robust and reduce production complexity, a stator flux bridge (FB) can be included, consequent in a single-unit stator. Adding an FB not just minimizes manufacturing complication and creates a stronger stator arrangement but also helps alleviate CT presented in Figure 12, include two possible locations to situation stator FB: the inner aspect (there the FB is inserted next to the stator pole) and the outer aspect (there the FB is inserted next to the stator yoke). Furthermore, the width of the FB is a different significant determinant connected to efficiency.

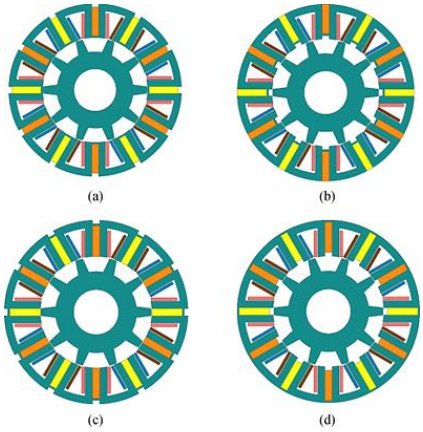

Figure 11. Finite element models of the proposed three-phase 12-slot/10-pole FSPM machines are illustrated as follows: (a) Inner stator with inner rotor, (b) Inner stator with outer rotor, (c) Outer stator with inner rotor, and (d) Outer stator with outer rotor, adapted from [43]

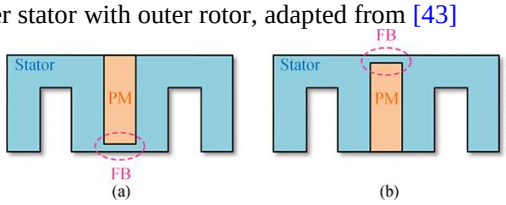

Figure 12. Location of the stator FB (a) Inner layer (b) Outer layer [43]

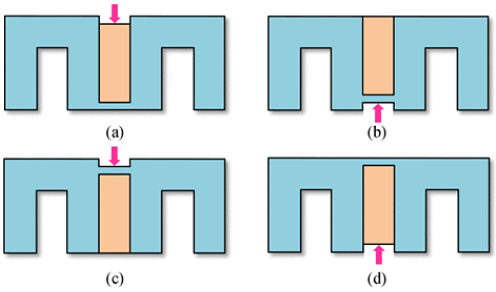

Figure 13. Four configurations of FSPM machines incorporating short permanent magnets and stator flux barriers are depicted: (a) Inner stator with inner rotor, (b) Inner stator with outer rotor, (c) Outer stator with inner rotor, and (d) Outer stator with outer rotor. [43]

Simulation results for CT in the inner/inner structure are presented for diverse PM dimensions illustrated in Figure 11(a) and 13(a). In such an arrangement, the stator FB is positioned on the inner aspect and the PM dimension decreases the inner axial axis. The result of the CT is illustrated in Figure 14(a).

Inner/outer structure is illustrated in Figure 11(b) and 13(b). This structure conclusion for CT is illustrated in Figure 14(b). Regarding this arrangement, the stator FB is included on the inner side, and the dimension of the PM is mitigated in the outer axial axis. When the PM dimension is mitigated to 17 mm, the peak significance of the CT decline to 40% of the 19 mm arrangement. Still, when the PM dimension is continuously decreased from 17 mm to 15 mm, only a slight decline in CT is detected. The CT with 17 mm PM dimension was diminished by 60% contrasted to 19 mm.

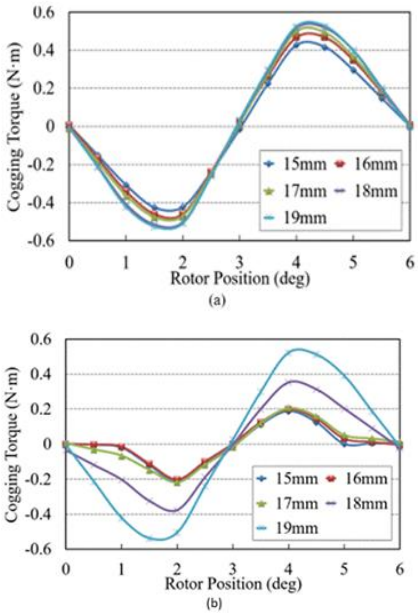

Figure 14. CT results a) CT illustration of the inner/inner structure b) CT illustration of the inner/outer structure [43]

The connection between CT and permanent magnet dimension in the outer/inner structure is illustrated in Figure 11(c) and 13(c). This structure outcomes CT is illustrated in Figure15(a). As the PM length decreases, the CT significantly reduces, reaching a minimum at a PM dimension of 15 mm. Reducing the PM dimension from 19 mm to 15 mm outcomes in a continuous diminish in average output torque; even so, this diminution is more limited compared to the inner/outer structure.

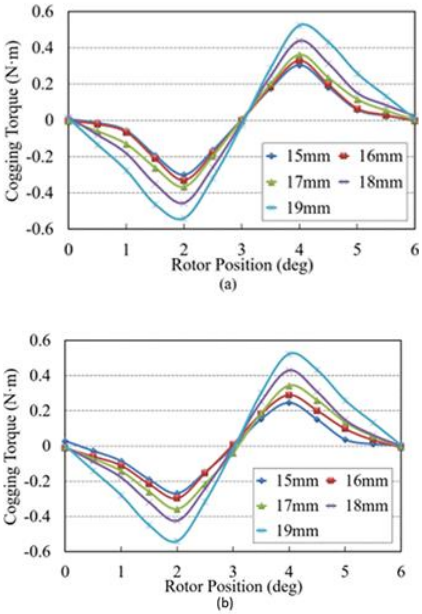

Figure 15. CT a) CT illustration of the outer/inner structure b) CT illustration of the outer/outer structure [43]

Within the outer/outer structure, the stator FB is included on the outer aspect, and the PM dimension is decreased to the outer axial bearing, as illustration in Figure 11(d) and 13(d). In this topology, the CT is displayed in Figure 15(b). As the PM dimension decreases, the CT declines. Additionally, in the topology with a PM length of 17 mm, the peak significance of the CT is minimized by 34% compared to the design with a PM dimension of 19 mm, although the torque loss is 13%.

Stator PM motors, especially FSPM dual salient PM, and flux inverted PM motors, are gaining increasing attention in various fields such as EVs [52,53], wind power transformation [54], and wave power transformation [55]. These motors share common structural features, such as the existence of PMs and core turns in the stator, and the rotor condition created as a basic iron core. These characteristics facilitate easy heat management of the PMs and provide a simple and robust structure for the rotor. Traditional stator PM motors utilize non-overlapping concentrated armature windings, resulting in low winding resistance and low copper consumption. However, this design has limitations in improving power density further. [45]

Du et al. [45] focused on the armature winding configuration pattern of FSPM motors (FSPMMs). In their study, the air-gap PM flux density of an existing 12s/10p FSPMM was analyzed, and a new 12s/7p FSPMM was proposed. Unlike the traditional non-overlapping concentrated winding, the new motor was designed with a distributed winding configuration to enhance torque density. The results were verified by calculating and analyzing the electromagnetic characteristics of both motors, and conclusions were drawn based on the findings.

Figure 16 demonstrates the configuration of a conventional 12/10-pole FSPMM, referred to as Motor I in this article. This motor's stator features essential teeth would with non-overlapping compact windings made from U-shaped layered parts, among which the permanent magnets are sandwiched, with their magnetic alignment courses configured alternately and adjacent in the tangential direction.

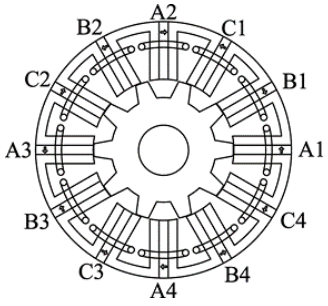

Figure 16. Motor I – 12s/10p FSPMM [45]

The winding factor of the motor designated Motor II displayed in Figure 17(a) will be quite low. Thus, with the aim of increase the power density, the distributed winding called Motor III shown in Figure 17(b) is preferred. Therefore, according to the proposed winding design method, there is only one type of winding configuration for 12/10 pole FSPM motors and two types of winding configurations for 12/7 pole FSPM motors.

The rotor also comprises of a basic iron core thought significant teeth.

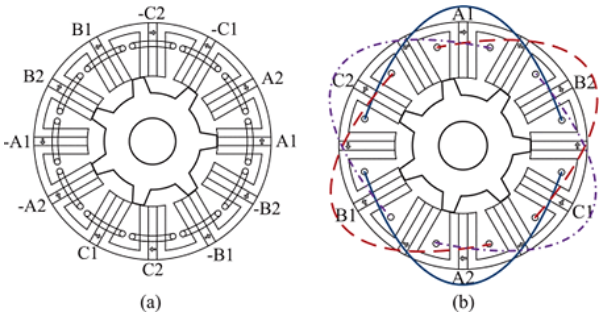

Figure 17. Armature winding connection of 12s/7p FSPMM. (a) Motor II-Classic non-overlapping winding (b) Motor III – Spread winding [45]

Displayed in Figure 18 are the CT waveforms for these motors. The peak to peak magnitude of CT for the 12s/7p FSPMM is 0.62 Nm as observed, which constitutes only 24.5% of the corresponding value for the 12s/10p FSPMM. This significant decrease in CT is one of the factors contributing to the reduced torque variation exhibited by Motor III.

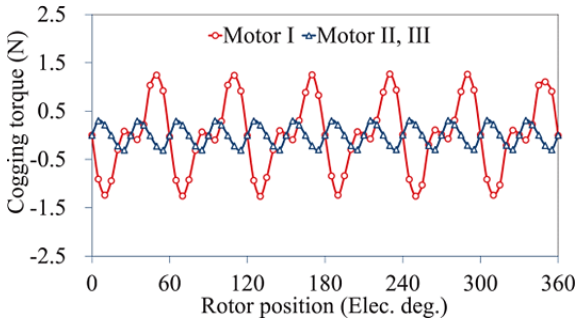

Figure 18. CT waveforms of three motors [45]

The use of distributed winding has been found to significantly boost the power density of the 12s/7p FSPMM contrasted to the motor with non-overlapping dense winding. Additionally, it has been observed that the 12s/7p FSPM motor exhibits a lower CT compared to its 12s/10p counterpart. However, the average value of the coil inductance of the 12s/7p FSPMM with distributed winding is more than four periods that of the other two motors. Finally, a prototype of a 12s/10p FSPMM was developed and evaluated. The trial outcomes, including the three-phase no-load EMF and three-phase self-inductance, have verified the outcomes derived from FEA and the investigative design.

Lan et al. [49], two surface-mounted PMSM prototypes with different magnetic loading levels were examined M1 (10-pole/12-slot, low magnetic loading) and M2 (12-pole/18-slot, high magnetic loading), as illustrated in Figure 19. The aim was to evaluate the influence of dummy slots on machine performance.

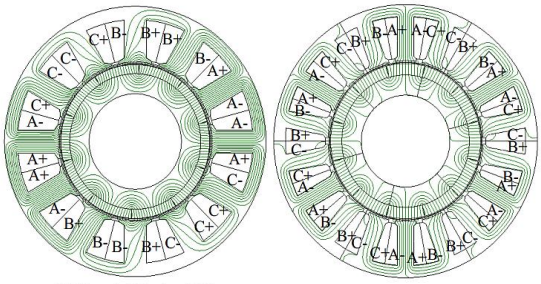

Figure 19. Stator winding configuration and flux path in the no-load state.[49]

According to the results, dummy slots impact not only the harmonic components of the CT but also the distribution of local forces on the stator bore. These effects stem from alterations in the air-gap flux density caused by the presence of dummy slots. The main goal of incorporating dummy slots is to reduce the amplitude of CT, considered a global force.

The paper presents a mathematical model for CT generated by real slots and extends it by formulating the additional torque contributions introduced by dummy slots. The total CT is defined as the sum of both components. Although certain harmonics can theoretically be cancelled through dummy slot placement, the cancellation is not perfect due to differences in the behavior of real and dummy slots.

In practice, one dummy slot was applied to each tooth in the M1 machine, and two were used in M2, as shown in Figure 20. This led to a notable reduction in the fundamental CT in both machines. However, some higher-order components increased specifically the 24th harmonic in M1 and the 18th in M2 (shown Figure 21).

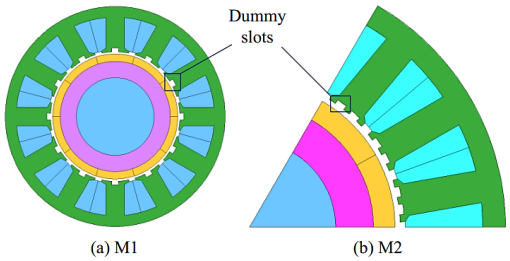

Figure 20. Electromagnetic finite element models of M1 and M2 incorporating dummy slots.[49]

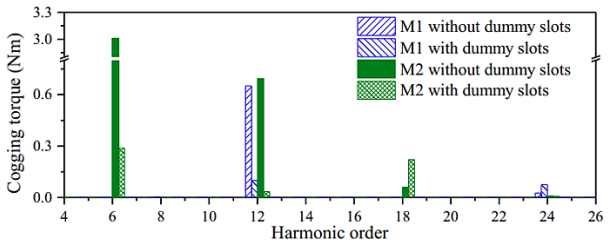

Figure 21. Spectral analysis. [49]

Overall, the study highlights how dummy slots alter CT harmonics and emphasizes their implications for noise and vibration performance.

In this study [50], Yokoi and Higuchi proposed and analyzed various techniques aimed at reducing CT in surface-mounted PM synchronous motors (SPMSMs). The first method presented involves an “Alternate Slot Winding” configuration, in which the windings and stator slots are arranged in an alternating pattern. This structure was primarily developed to suppress torque ripple components caused by back electromotive force (EMF). However, due to the irregular slot configuration, the frequency of CT is halved, which may, in turn, negatively influence torque ripple behavior.

To address this issue, the stator design with alternate slots was enhanced by the inclusion of "Dummy Slots," as illustrated in Figure 22. These dummy slots were constructed to replicate the magnetic reluctance distribution of the actual slots. As a result, they effectively suppress the lowest-order harmonic components of CT. The slot opening widths for both real and dummy slots were adjusted to be half the length of the slot pitch. This configuration enhances the presence of higher-order harmonics, thereby contributing to the reduction of torque ripple.

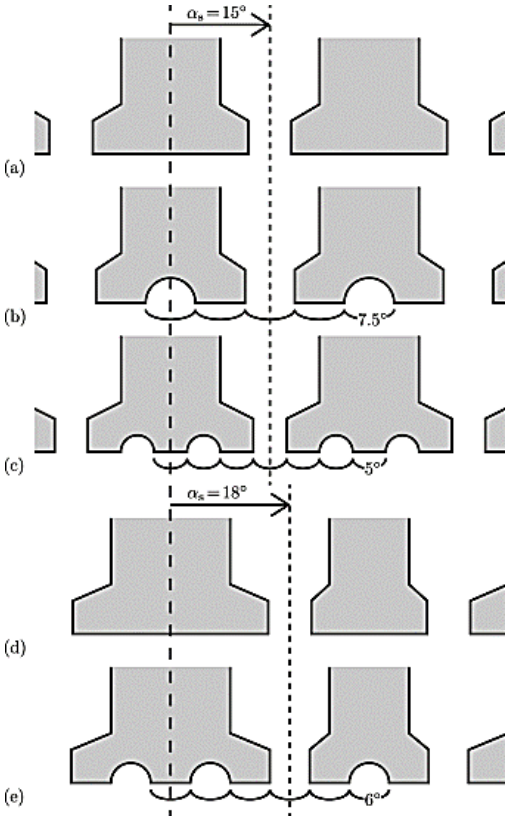

Figure 22. Illustrations depict the configurations of both actual and dummy stator slots for equal and alternate slot winding arrangements. The angular positions are presented in terms of electrical degrees. Specifically, subfigures include: (a) Equal Slot Winding with 24 slots (ESW24), (b) ESW48, (c) ESW72, (d) Alternate Slot Winding with 24 slots (ASW24), and (e) ASW60. [50]

Moreover, the rotor magnet design was considered alongside the stator structure. Two principal strategies were implemented to minimize torque pulsations. The first approach involved shifting the positions of the magnets on the rotor surface by a specific angle. This technique particularly aims to mitigate dominant CT harmonics, such as the 30th-order component. A theoretical expression was also provided to determine which harmonic component should be targeted for suppression. The second approach consisted of modifying the magnet arc width, primarily to attenuate undesirable back-EMF harmonics such as the 7th order. While this method primarily improves the EMF profile, it also contributes indirectly to the reduction of CT.

Ultimately, the study emphasized that effective CT reduction can be achieved through the combined application of multiple design techniques, each addressing different harmonic components, as demonstrated in the simulation results (Figure 23). The integration of alternate slot windings, dummy slots, and optimized rotor magnet arrangements was shown to significantly decrease torque ripple. The effectiveness of the suggested methods was confirmed through FEM analyses.

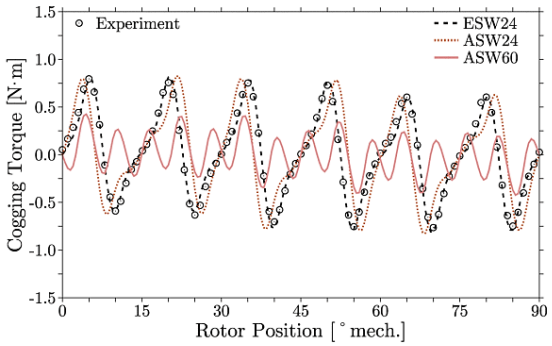

Figure 23. CT for ESW24, ASW24, and ASW60. [50]

In a study conducted by Zhu et al. [51], three innovative designs of hybrid excited multi-tooth flux-switching permanent magnet (HE-MFSPM) machines were proposed. These designs integrate the benefits of hybrid excitation with those of multi-tooth stator FSPMM's. While all three models operate on a similar principle, they differ significantly in the configuration of their stator structures.

As illustrated in Figure 24, Models I, II, and III feature hybrid excitation systems comprising tangentially magnetized permanent magnets and concentrated field windings (FWs). Model I stands out as the design utilizing the least amount of PM material, employing auxiliary slots and tangential magnets with opposing polarities. Model II incorporates radially magnetized PMs within the auxiliary slots and shares an equal PM volume with Model III. Notably, Model III enhances system reliability and modularity through the inclusion of six fault-tolerant teeth.

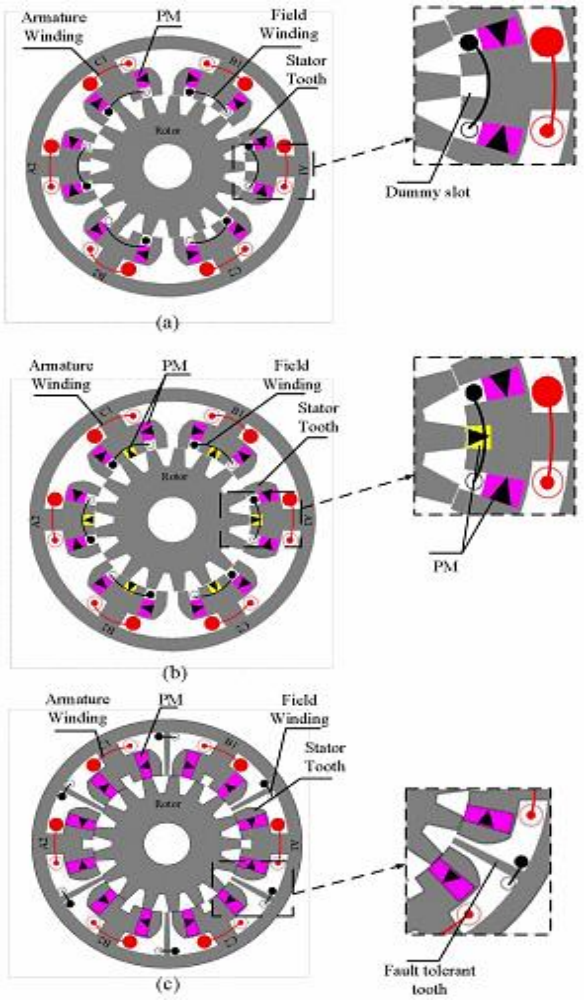

Figure 24. Structures of three HE-MFSPMM's. (a) Model I. (b) Model II. (c) Model III.[51]

To ensure effective flux control and mitigate the risk of demagnetization, all designs utilize a parallel hybrid excitation approach that separates the magnetic paths of PMs and FWs. Two-dimensional finite element analysis (2-D FEA) confirms that magnetic flux follows the intended excitation source when activated independently. The fault-tolerant structure of Model III, in particular, restricts inter-phase flux coupling, thereby improving phase separation.

The analysis demonstrated that all three HE-MFSPM configurations exhibit low CT characteristics. Among them, Model I achieved the minimum peak-to-peak CT, while Model III followed closely behind. Figure 25 presents the CT waveforms for the three machines, offering a comparative visual overview of their torque behavior. Overall, the study concludes that all models deliver favorable CT performance, with Model I emerging as the most effective in this regard.

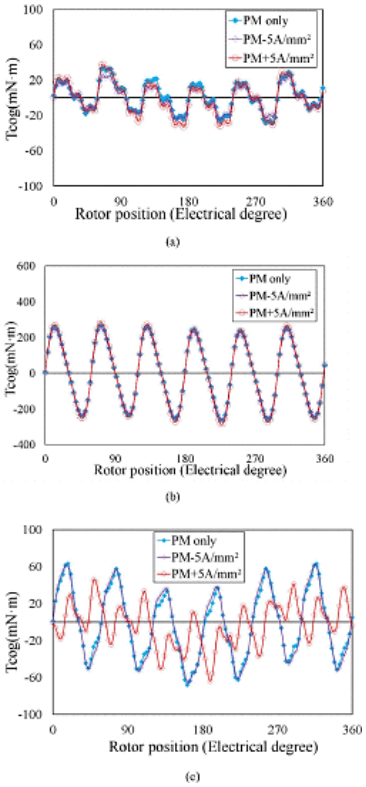

Figure 25. CT waveforms of three he-mfspm machines. (a) Model I. (b) Model II. (c) Model III. [51]

3.3 Rotor and stator side adjustment

In this section, the methods employed to minimize CT in FSPMMs will be examined, focusing on both rotor and stator components. Through various optimization techniques and structural modifications, improvements made collaboratively in the configurations of the rotor and stator support the mitigation of CT. A comprehensive summary of these methods, along with their related references, is presented in Table 4 to facilitate a clearer understanding of the applied strategies.

Table 4. Rotor and stator side adjustments

ROTOR-STATOR ADJUSTMENT	REFERENCE
tooth chamfering methods	[56]
Improvement of stator and rotor teeth	[17,57]
Slot-pole combination, stator-poles and rotor-teeth (P-T) combinations	[58,59]
Slot pitch of the stator and rotor, magnet arc, stator tooth arc, and stator yoke thickness	[60]
Rotor/stator configurations	[61,62,63]
Including arrangements of stator slots and rotor poles skewing angle stator tooth width rotor tooth width magnet thickness	[64,65]
cos-formed edge rotor (CSER), cos-formed edge stator, and dual cos-formed edge, air-gap field modulation	[66]

Zhu et. al. [56], various tooth chamfering methods are proposed to minimize CT for a 12/10 FSPMM. The effects of both round beads and correct angles, as well as their possible arrangements, on CT are examined using 2D FEA. The finding of the research show that using the right angles on both stator and rotor teeth is the most productive process. The combinations are illustrated in Figure 26.

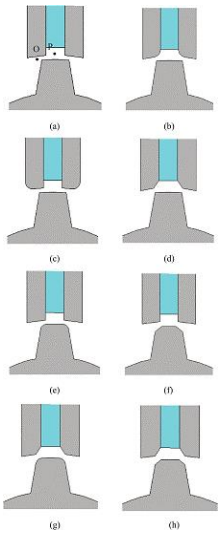

Figure 26. Various tooth chamfering configurations applied to both stator and rotor teeth are presented as follows: (a) Original design, (b) Stator tooth with a round fillet on the magnet side, (c) Stator tooth with a round fillet on the slot side, (d) Stator tooth with a right angle on the magnet side, (e) Rotor tooth with a round fillet, (f) Rotor tooth with a right angle, (g) Stator tooth with a right angle and rotor tooth with a round fillet, (h) Right-angled chamfering applied to both stator and rotor teeth [56]

In order to provide a clearer explanation of this phenomenon, an analysis of the flux density in the air gap has been conducted. Additionally, the effects on phase back electromotive force and electromagnetic torque have been thoroughly analyzed. The expected conclusions show that the suggested method can considerably reduce the peak value of CT from 2.6 Nm to 0.4 Nm, with only a 1.6% reduction in average torque. These findings represent a notable improvement when compared to approaches utilized in the previous literature.

First, the CT waveforms for the initial design of the 12/10 FSPMM, based on 2D-FEA, are displayed in Figure 27, where the peak torque magnitude reaches 5.2 Nm with a mechanical period of 6°. It is concluded that using a circular bead has very little effect on CT and that simply adding a circular bead does not reduce the torque. However, employing a right angle on the magnet section of the stator tooth lowers the torque partially. When examining the effects of the circular fillet and the right angle, it is determined that the CT in the rotor tooth can be considerably reduced with the right angle, that is more productive than the round bead. Comparisons of diverse configurations also indicate that the configuration utilizing both right angles provides the best solution.

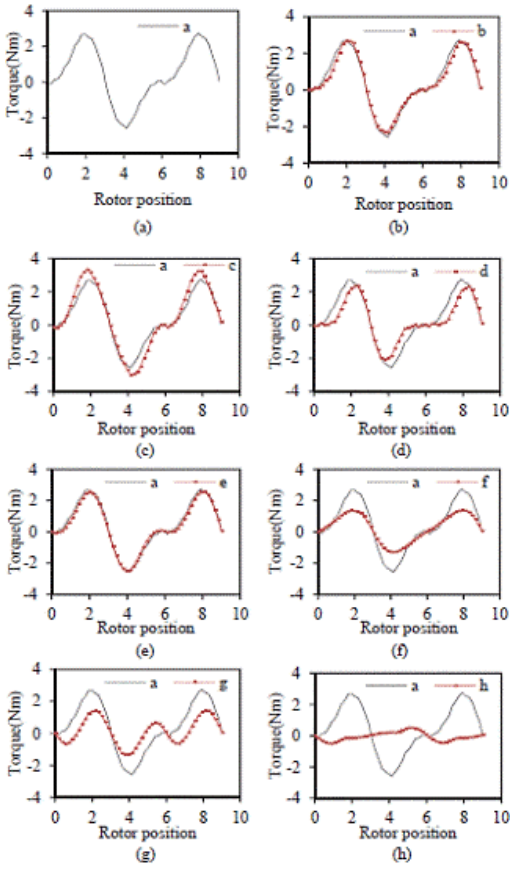

Figure 27. CT waveforms of diverse tooth-chamfering configurations. (a) Initial (b) round fillet in stator tooth/ magnet side, (c) round fillet in stator tooth/slot side, (d) right angle in stator tooth / magnet side, (e) round fillet in rotor tooth, (f) right angle in rotor tooth, (g) right angle in stator tooth / round fillet in rotor tooth, (h) right angles in both stator and rotor teeth [56]

In this section, the optimization studies carried out for the reduction of CT in the rotor and stator components of the FSPM electric machines studied are comprehensively discussed. These optimization processes include various design changes to refine the efficiency of the machine and diminish vibrations. The applications of the related optimizations are visualized with a detailed diagram in Figure 28.

4 Conclusion

A range of methods aimed at reduce CT in FSPM machines have been explored in this study. CT is an undesirable effect that occurs at low-speed operation of the motor and adversely impacts the overall performance of the system. The conducted analyses and implementations have demonstrated the effectiveness of the techniques used to minimize CT.

Among the methods examined are the optimization of magnet arrangement and modifications to the rotor and stator geometry. The combination of these techniques has significantly reduced the CT while contributing to have more stable operation and increased efficiency of the motor. In conclusion, the studies conducted to reduce CT are critically important for ensuring high performance and reliability in industrial applications of FSPMM. Future research is expected to contribute a significant advancement in this field through more innovative design and control methods.

Despite the progress in reducing CT through various design and control strategies, several challenges remain. One of the key difficulties lies in achieving optimal torque performance without compromising other machine parameters such as cost, manufacturability, and thermal behavior. Moreover, while many studies have focused on specific structural modifications, comprehensive comparisons across different mitigation techniques are still limited. In particular, there is a noticeable gap in the literature regarding integrated approaches that simultaneously consider electromagnetic, thermal, and mechanical aspects. Therefore, future work should aim to address these multidimensional challenges by combining advanced modeling techniques with practical validations.

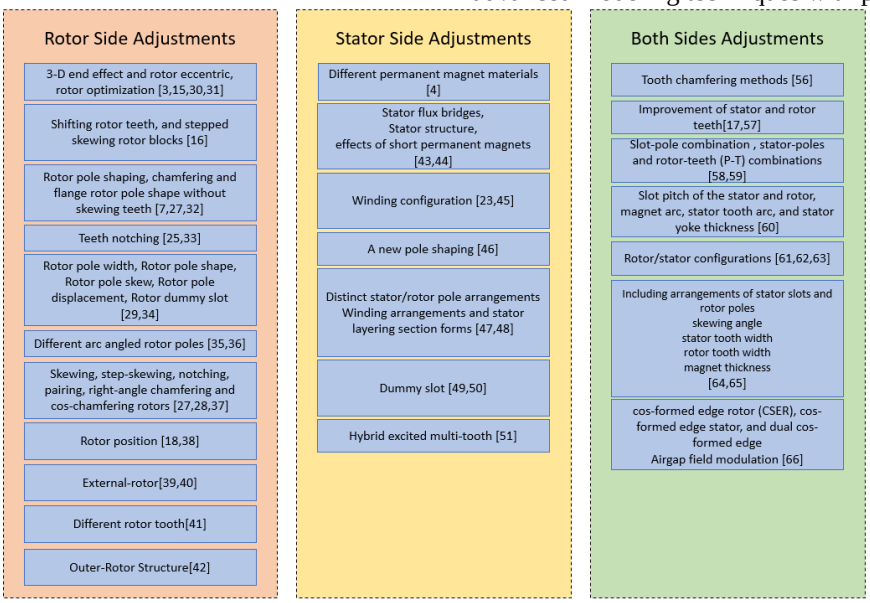

Figure 28. Classification of structural optimization techniques for CT reduction in FSPM machines

Acknowledgement

This work was supported by TÜBİTAK under project number 124E478. The authors would like to express their gratitude for the financial and technical support provided.

Conflict of Interest

The authors declare that there is no conflict of interest.

Similarity Rate (iThenticate): 19%

References

[1] P. Svetlik, K. Hruska, Construction of the FSPM machine and its measurement in comparison with modeled results, 2016 18th European Conference on Power Electronics and Applications (EPE'16 ECCE Europe), pp. 1-9, 2016.

[2] H. Chen, A. M. EL-Refaie and N. A. O. Demerdash, Flux-Switching Permanent Magnet Machines: A Review of Opportunities and Challenges—Part I: Fundamentals and Topologies, in IEEE Transactions on Energy Conversion, vol. 35, no. 2, pp. 684-698, June 2020, doi: 10.1109/TEC.2019.2956600

[3] W. Hua, G. Zhang, M. Cheng, Investigation and Design of a High-Power Flux-Switching Permanent Magnet Machine for Hybrid Electric Vehicles, in IEEE Transactions on Magnetics, vol. 51, no. 3, pp. 1-5, Art no. 8201805, March 2015. doi: 10.1109/TMAG.2014.2345732

[4] M. Taha, A. A. Saleh, A. Hemeida, Effect of Magnet Materials on Designing of a High Power-Low Voltage Permanent Magnet Flux Switching Motor for Automotive Applications, 2020 International Conference on Electrical Machines (ICEM), pp. 2280-2286, 2020.

[5] Z. Xiang, L. Quan, X. Zhu, A New Partitioned-Rotor Flux-Switching Permanent Magnet Motor with High Torque Density and Improved Magnet Utilization, in IEEE Transactions on Applied Superconductivity, vol. 26, no. 4, pp. 1-5, Art no. 5201905 June 2016. doi: 10.1109/TASC.2016.2514486

[6] L. Hao, M. Lin, D. Xu, W. Zhang, N. Li, Rotor design techniques for reducing the CT in a novel dual-rotor axial field flux-switching permanent magnet machine, 2014 17th International Conference on Electrical Machines and Systems (ICEMS), pp. 1581-1586, 2014.

[7] W. Hua, M. Cheng, Z. Q. Zhu, D. Howe, Analysis and Optimization of Back EMF Waveform of a Flux-Switching Permanent Magnet Motor, in IEEE Transactions on Energy Conversion, vol. 23, no. 3, pp. 727-733, Sept. 2008. doi: 10.1109/IEMDC.2007.382817

[8] X. Zhu, W. Hua, Back-EMF waveform optimization of flux-switching permanent magnet machines, 2016 XXII International Conference on Electrical Machines (ICEM), pp. 2419-2425, 2016.

[9] Z. Q. Zhu, A. S. Thomas, J. T. Chen and G. W. Jewell, CT in Flux-Switching Permanent Magnet Machines, in IEEE Transactions on Magnetics, vol. 45, no. 10, pp. 4708-4711, Oct. 2009. doi: 10.1109/TMAG.2009.2022050

[10] C. Sikder, I. Husain, W. Ouyang, CT Reduction in Flux-Switching Permanent-Magnet Machines by Rotor Pole Shaping, in IEEE Transactions on Industry Applications, vol. 51, no. 5, pp. 3609-3619, Sept.-Oct. 2015. doi: 10.1109/TIA.2015.2416238

[11] I. Hussain, F. Khan, U. Zafar, N. Ahmad, N. Iqbal, CT reduction of flux-switching permanent magnet machine with overlapping windings, 2018 1st International Conference on Power, Energy and Smart Grid (ICPESG), pp. 1-6, 2018.

[12] Mengjie Shen, Jianhua Wu, Chun Gan, Yihua Hu, Wenping Cao, CT reduction in FSPM machines with short magnets and stator lamination bridge structure, IECON 2016 - 42nd Annual Conference of the IEEE Industrial Electronics Society, pp. 4307-4312, 2016.

[13] E. Cetin, Z. Q. Zhu, Optimization of Torque Performance of FSPM Machines by Rotor Pole Shaping using FEA and Genetic Algorithm, 2022 Second International Conference on Sustainable Mobility Applications, Renewables and Technology (SMART), pp. 1-8, 2022.

[14] J. H. Kim, Y. Li, E. Cetin, B. Sarlioglu, CT minimization with rotor tooth shaping in axial flux-switching permanent magnet machine, 2016 IEEE Energy Conversion Congress and Exposition (ECCE), pp. 1-7, 2016.

[15] J. Zhao, Y. Yan, B. Li, X. Liu, Z. Chen, Influence of Different Rotor Teeth Shapes on the Performance of Flux Switching Permanent Magnet Machines Used for Electric Vehicles, Energies 7, 8056-8075, 2014. doi:10.3390/en7128056

[16] X. Zhu, W. Hua, CT Suppression in Flux-Switching Permanent Magnet Machines by Superposition of Single Rotor Tooth, 2018 IEEE Energy Conversion Congress and Exposition (ECCE), pp. 4359-4366, 2018.

[17] X. Zhu, W. Hua, G. Zhang, Analysis and Reduction of CT for Flux-Switching Permanent Magnet Machines, in IEEE Transactions on Industry Applications, vol. 55, no. 6, pp. 5854-5864, Nov.-Dec. 2019. doi: 10.1109/TIA.2019.2938721

[18] A. Lindner, H. Kurtović, I. Hahn, Investigation of parametrized curves for the pole shaping in an E-core Flux-Switching Machine with large air-gap, 8th IET International Conference on Power Electronics, Machines and Drives (PEMD 2016), pp. 1-5, 2016.

[19] J. Zhao, Y. Zheng, C. Zhu, H. Chen and L. Yang, Torque ripple reduction of a modular-stator outer-rotor flux-switching permanent-magnet motor, IECON 2017 - 43rd Annual Conference of the IEEE Industrial Electronics Society, pp. 3765-3770, 2017.

[20] F. Yu, M. Cheng, K. T. Chau, Controllability and Performance of a Nine-Phase FSPM Motor Under Severe Five Open-Phase Fault Conditions, in IEEE Transactions on Energy Conversion, vol. 31, no. 1, pp.

323-332, March 2016. doi: 10.1109/TEC.2015.2486521
[21] W. Huang, W. Hua, X. Zhu, Y. Fan, M. Cheng, Comparison of CT Compensation Methods for a Flux-Switching Permanent Magnet Motor by Harmonic Current Injection and Iterative Learning Control, 2020 International Conference on Electrical Machines (ICEM), pp. 1971-1977, 2020.
[22] M. Cheng, P. Han, Y. Du, H. Wen, X. Li, A Tutorial on General Air-Gap Field Modulation Theory for Electrical Machines, in IEEE Journal of Emerging and Selected Topics in Power Electronics, vol. 10, no. 2, pp. 1712-1732, April 2022. doi: 10.1109/JESTPE.2021.3055224
[23] Q. Ding, T. Ni, X. Wang, Z. Deng, Optimal Winding Configuration of Bearingless Flux-Switching Permanent Magnet Motor with Stacked Structure, in IEEE Transactions on Energy Conversion, vol. 33, no. 1, pp. 78-86, March 2018. doi: 10.1109/TEC.2017.2752746
[24] P. Wang, W. Hua, G. Zhang, B. Wang and M. Cheng, Torque Ripple irradi Suppression of Flux-Switching Permanent Magnet Machine Based on General Air-Gap Field Modulation Theory, in IEEE Transactions on Industrial Electronics, vol. 69, no. 12, pp. 12379-12389, Dec. 2022. doi: 10.1109/TIE.2021.3137617
[25] D. Wang, X. Wang, S. -Y. Jung, Reduction on CT in Flux-Switching Permanent Magnet Machine by Teeth Notching Schemes, in IEEE Transactions on Magnetics, vol. 48, no. 11, pp. 4228-4231, Nov. 2012. doi: 10.1109/TMAG.2012.2200237
[26] D. Xie, Y. Wang, Z. Deng, FSPM machines with twisted-rotor structure, 2014 9th IEEE Conference on Industrial Electronics and Applications, pp. 1533-1538, 2014.
[27] W. Fei, P. C. K. Luk, J. X. Shen, B. Xia and Y. Wang, Permanent-Magnet Flux-Switching Integrated Starter Generator with Different Rotor Configurations for CT and Torque Ripple Mitigations, in IEEE Transactions on Industry Applications, vol. 47, no. 3, pp. 1247-1256, May-June 2011. doi: 10.1109/ECCE.2010.5618119
[28] S. M. K. Sangdehi, S. E. Abdollahi, S. A. Gholamian, CT Reduction of 6/13 Hybrid Excited Flux Switching Machine with Rotor Step Skewing, 2019 5th Conference on Knowledge Based Engineering and Innovation (KBEI), Tehran, Iran, pp. 582-586, 2019.
[29] L. Hao, M. Lin, D. Xu, W. Zhang, N. Li, Rotor design techniques for reducing the CT in a novel dual-rotor axial field flux-switching permanent magnet machine, 2014 17th International Conference on Electrical Machines and Systems (ICEMS), pp. 1581-1586, 2014.
[30] Z. Ma, M. Cheng, W. Yu, Y. Jiang, W. Hua, C. Zhao, Exploration of Rotor Topology Evolution Mechanism in the Stator-PM Machines, in IEEE Transactions on Industry Applications, 2024. doi: 10.1109/TIA.2024.3481398
[31] X. Zhu, Z. Xiang, C. Zhang, L. Quan, Y. Du, W. Gu, Co-Reduction of Torque Ripple for Outer Rotor Flux-Switching PM Motor Using Systematic Multi-Level Design and Control Schemes, in IEEE Transactions on Industrial Electronics, vol. 64, no. 2, pp. 1102-1112, Feb. 2017. doi: 10.1109/TIE.2016.2613058
[32] J. Xiu, S. Wang, Y. Xiu, Reducing CT of 6/4 pole FSPM machine by optimising parameters of chamfering and flange rotor pole shape without skewing teeth, IET Electric Power Applications, 13: 277-284, 2019. doi:10.1049/iet-epa.2018.5435
[33] L. Hao, M. Lin, D. Xu, N. Li, W. Zhang, CT reduction of axial field flux-switching permanent magnet machine by rotor tooth notching, 2015 IEEE International Magnetics Conference (INTERMAG), pp. 1-1, 2015.
[34] M. Liu, W. Sixel, H. Ding, B. Sarlioglu, Investigation of Rotor Structure Influence on the Windage Loss and Efficiency of FSPM Machine, 2018 IEEE Energy Conversion Congress and Exposition (ECCE), Portland, pp. 6499-6505, 2018.
[35] E. Çetin, The Effects of the Unequal Rotor Slot Arc on CT for Flux Switching Permanent Magnet Machines, El-Cezeri Journal of Science and Engineering, vol. 11, no. 1, pp. 74–81, 2024. doi:10.31202/ecjse.1347168
[36] E. Cetin, CT reduction by utilizing the unequal rotor slot arc method for FSPM Machines, Ain Shams Engineering Journal, 2024. doi: 10.1016/j.asej.2024.103008
[37] Z. Zhang, P. Wang, W. Hua, T. Zhang, G. Wang, M. Hu, Comprehensive Investigation and Evaluation of CT Suppression Techniques of Flux-Switching Permanent Magnet Machines, in IEEE Transactions on Transportation Electrification, vol. 9, no. 3, pp. 3894-3907, Sept. 2023. doi: 10.1109/TTE.2023.3248220
[38] J. Zhao, W. Fu, Y. Zheng, Z. Chen, Y. Wang, Comparative Study of Modular-Stator and Conventional Outer-Rotor Flux-Switching Permanent-Magnet Motors, in IEEE Access, vol. 7, pp. 38297-38305, 2019. doi: 10.1109/ACCESS.2018.2890163
[39] W. Yu, K. Liu, W. Hua, M. Hu, Z. Zhang and J. Hu, A New High-Speed Dual-Stator Flux Switching Permanent Magnet Machine with Distributed Winding, in IEEE Transactions on Magnetics, vol. 58, no. 2, pp. 1-6, Art no. 8102006, 2022. doi: 10.1109/TMAG.2021.3082931
[40] Zuo, Zijie, Yidong Du, and Lei Yu. Influence of Stator/Rotor Torque Ratio on Torque Performance in External-Rotor Dual-Armature Flux-Switching PM Machines Machines 12, no. 9: 588, 2024. doi: 10.3390/machines12090588
[41] P. Su, Y. Wang, Y. Li, W. Hua and Y. Shen, CT Reduction of Axial-Modular Flux Switching Permanent Magnet Machine by Module Combination Technique, in IEEE Transactions on Transportation Electrification, vol. 10, no. 1, pp. 1947-1956, March 2024, doi: 10.1109/TTE.2023.3262845.
[42] Z. Xu, M. Cheng and M. Tong, Design Consideration for E-Core Outer-Rotor Flux-Switching Permanent Magnet Machines From the Perspective of the Stator-Poles and Rotor-Teeth Combinations, in IEEE Transactions on Industry Applications, vol. 61, no. 1,

pp. 161-171, Jan.-Feb. 2025, doi: 10.1109/TIA.2024.3478173

[43] C. Gan, J. Wu, M. Shen, W. Kong, Y. Hu, W. Cao, Investigation of Short Permanent Magnet and Stator Flux Bridge Effects on CT Mitigation in FSPM Machines, in IEEE Transactions on Energy Conversion, vol. 33, no. 2, pp. 845-855, June 2018. doi: 10.1109/TEC.2017.2777468

[44] X. Zhu, Z. Shu, L. Quan, Z. Xiang, X. Pan, Design and Multicondition Comparison of Two Outer-Rotor Flux-Switching Permanent-Magnet Motors for In-Wheel Traction Applications, in IEEE Transactions on Industrial Electronics, vol. 64, no. 8, pp. 6137-6148, Aug. 2017. doi: 10.1109/TIE.2017.2682025

[45] Y. Du, F. Xiao, W. Hua, X. Zhu, M. Cheng, L. Quan, K. T. Chau, Comparison of Flux-Switching PM Motors with Different Winding Configurations Using Magnetic Gearing Principle, in IEEE Transactions on Magnetics, vol. 52, no. 5, pp. 1-8, Art no. 8201908, 2016. doi: 10.1109/TMAG.2015.2513742

[46] C. Sikder, I. Husain, Stator vibration and acoustic noise analysis of FSPM for a low-noise design, 2016 IEEE Energy Conversion Congress and Exposition (ECCE), Milwaukee, WI, USA, pp. 1-8, 2016.

[47] Z. Z. Wu, Z. Q. Zhu, Analysis of Air-Gap Field Modulation and Magnetic Gearing Effects in Switched Flux Permanent Magnet Machines, in IEEE Transactions on Magnetics, vol. 51, no. 5, pp. 1-12, Art no. 8105012, 2015. doi: 10.1109/TMAG.2015.2402201

[48] A. Zohoori, A. Vahedi, M. A. Noroozi, Design study of FSPM generator with novel outer rotor configuration for small wind turbine application, 2014 14th International Conference on Environment and Electrical Engineering, pp. 275-279, 2014

[49] H. Lan, Q. Chen, J. Zou, Y. Xu, M. Wang and M. Liu, Influence of dummy slots on noise and vibration performance in permanent magnet synchronous machines, 2017 IEEE Transportation Electrification Conference and Expo, Asia-Pacific (ITEC Asia-Pacific), Harbin, China, 2017, pp. 1-6, doi: 10.1109/ITEC-AP.2017.8080970

[50] Y. Yokoi and T. Higuchi, Stator Design of Alternate Slot Winding for Reducing Torque Pulsation With Magnet Designs in Surface-Mounted Permanent Magnet Motors, in IEEE Transactions on Magnetics, vol. 51, no. 6, pp. 1-11, June 2015, Art no. 8202911, doi: 10.1109/TMAG.2015.2394771.

[51] Z. Jin, X. Zhu, S. Chen, Z. Li and S. Ding, Comparative Study on Three Novel Hybrid Excited Multitooth Flux-switching Permanent Magnet Machines, 2022 Joint MMM-Intermag Conference (INTERMAG), New Orleans, LA, USA, 2022, pp. 1-6, doi: 10.1109/INTERMAG39746.2022.9827848.

[52] K. T. Chau, C. C. Chan, C. Liu, Overview of permanent-magnet brushless drives for electric and hybrid electric vehicles, IEEE Trans. Ind. Electron., vol. 55, no. 6, pp. 2246–2257, Jun. 2008. doi: 10.1109/TIE.2008.918403

[53] L. Mo, L. Quan, X. Zhu, Y. Chen, H. Qiu, K. T. Chau, Comparison and analysis of flux-switching permanent-magnet double-rotor machine with 4QT used for HEV, IEEE Trans. Magn., vol. 50, no. 11, Art. ID 8205804, 2014. doi: 10.1109/TMAG.2014.2331313

[54] J. Zhang, Z. Chen, M. Cheng, Design and comparison of a novel stator interior permanent magnet generator for direct-drive wind turbines, IET Renew. Power Generat., vol. 1, no. 4, pp. 203–210, Dec. 2007. doi:10.1049/iet-rpg:20070054

[55] M. Yu, W. Zhao, Y. Wang, X. Wang, Design and Optimization of a Novel Dual-Rotors Flux-Switching Permanent-Magnet Machine, 2020 IEEE 1st China International Youth Conference on Electrical Engineering (CIYCEE), pp. 1-6, 2020.

[56] X. Zhu, W. Hua, M. Cheng, CT minimization in flux-switching permanent magnet machines by tooth chamfering, 2016 IEEE Energy Conversion Congress and Exposition (ECCE), pp. 1-7, 2016

[57] S. Çarkıt, N. Üstkoyuncu, T. Çarkıt, Investigation of the effects of magnet, stator and rotor geometries on torque and torque ripple in permanent magnet flux switched motor, Gazi University Journal of Science Part C: Design and Technology, 308-314, 2024. doi:10.29109/gujsc.1202243.

[58] D. Bobba, Y. Li, B. Sarlioglu, “Harmonic Analysis of Low-Stator-Slot and Rotor-Pole Combination FSPM Machine Topology for High Speed,” in IEEE Transactions on Magnetics, vol. 51, no. 11, pp. 1-4, Art no. 8207104, 2015. doi: 10.1109/TMAG.2015.2446414

[59] Y. Shi, L. Jian, J. Wei, Z. Shao, W. Li, C. C. Chan, A New Perspective on the Operating Principle of Flux-Switching Permanent-Magnet Machines, in IEEE Transactions on Industrial Electronics, vol. 63, no. 3, pp. 1425-1437, March 2016. doi: 10.1109/TIE.2015.2492940

[60] J. Zhu, L. Wu, H. Wen, “Optimization and Comparison of Dual-Armature Flux-Switching Permanent Magnet Machines with Different Stator Core Shapes,” in IEEE Transactions on Industry Applications, vol. 58, no. 1, pp. 314-324, Jan.-Feb. 2022. doi: 10.1109/TIA.2021.3131300

[61] Y. Gu, L. Quan, Z. Xiang, Minimization the torque ripple of flux-switching permanent magnet motor based on iterative learning control, 2014 17th International Conference on Electrical Machines and Systems (ICEMS), pp. 1985-1989, 2014

[62] Z. Zhang, P. Wang, W. Hua, T. Zhang, G. Wang, M. Hu, Comprehensive Investigation and Evaluation of CT Suppression Techniques of Flux-Switching Permanent Magnet Machines, in IEEE Transactions on Transportation Electrification, vol. 9, no. 3, pp. 3894-3907, Sept. 2023. doi: 10.1109/TTE.2023.3248220

[63] L. Zhu, S. Z. Jiang, Z. Q. Zhu, C. C. Chan, Analytical Methods for Minimizing CT in Permanent-Magnet Machines, in IEEE Transactions on Magnetics, vol. 45, no. 4, pp. 2023-2031, April 2009. doi: 10.1109/TMAG.2008.2011363

[64] X. Zhu, W. Hua, Z. Wu, W. Huang, H. Zhang, M. Cheng, "Analytical Approach for Cogging Torque Reduction in Flux-Switching Permanent Magnet Machines Based on Magnetomotive Force-Permeance Model," in IEEE Transactions on Industrial Electronics, vol. 65, no. 3, pp. 1965-1979, March 2018. doi: 10.1109/TIE.2017.2739688

[65] Z. Gu, B. Zhao, R. Hu, X. Yin, X. Liu, Q. Zhang, J. Gong, N. Zhou, Y. Huang, "Electromagnetic Structure Research of the Modular Arc-Linear Flux Switching Permanent-Magnet Motor," 2018 21st International Conference on Electrical Machines and Systems (ICEMS), pp. 1857-1862, 2018

[66] P. Wang, W. Hua, G. Zhang, B. Wang, M. Cheng, Torque Ripple Suppression of Flux-Switching Permanent Magnet Machine Based on General Air-Gap Field Modulation Theory, in IEEE Transactions on Industrial Electronics, vol. 69, no. 12, pp. 12379-12389, Dec. 2022. doi: 10.1109/TIE.2021.3137617